Photoactivation of ROS production in situ transiently activates cell proliferation in mouse skin and in the hair follicle stem cell niche promoting hair growth and wound healing

Elisa Carrasco[1, 2, 3, #], María I. Calvo[1, 2, #], Alfonso Blázquez-Castro[1, 2, ^], Daniela Vecchio[3, 4], Alicia Zamarrón[2], Irma Joyce Dias de Almeida[1, 2], Juan C. Stockert[2], Michael R. Hamblin[3, 4, 5], Ángeles Juarranz[2], Jesús Espada[1, 2, #,*]

1. Instituto de Investigaciones Biomédicas "Alberto Sols", Departamento de Bioquímica, CSIC-Universidad Autónoma de Madrid, Arturo Duperier 4, 28029 Madrid, Spain
2. Departamento de Biología, Facultad de Ciencias, Universidad Autónoma de Madrid, Darwin 2, 28049 Madrid, Spain
3. Wellman Center for Photomedicine, Massachusetts General Hospital, Boston MA, 02114, USA
4. Department of Dermatology, Harvard Medical School, Boston MA, 02115, USA
5. Harvard-MIT Division of Health Sciences and Technology, Cambridge, MA, 02139, USA

Present address: Grupo de Dermatología Experimental, Instituto Ramón y Cajal de Investigaciones Sanitarias, Fundación para la Investigación Biomédica Hospital Universitario Ramón y Cajal, Carretera Colmenar Viejo Km 9.100, 28034 Madrid, Spain

^ Present address: Aarhus Institute of Advanced Studies (AIAS), Høegh-Guldbergs Gade 6B Building 1630, room 113, 8000 Aarhus C, Denmark

*Correspondence to: Jesús Espada (jespada@iib.uam.es)

Fax: +0034 585 4400

Tlf.: +0034 585 4401

Short title: *In vivo* stem cell activation by ROS

Abbreviations: ROS (Reactive Oxygen Species); HF (Fair Follicle); HS (Hair Shaft); SG: (Sebaceous Gland); Bg (Bulge Region); DP (Dermal Papilla); PpIX (Protoporphyrin IX); LRC (Label Retaining Cells); mALA (methyl aminolevulinate); PT (phototreatment); hET (2-hydroxyethidium); DHF-DA (2′,7′-dichlorodihydrofluorescein diacetate); NAC (N-acetylcysteine); AA (ascorbic acid)

ABSTRACT

The role of reactive oxygen species (ROS) in the regulation of hair follicle cycle and skin homeostasis is poorly characterized. ROS have been traditionally linked to human disease and ageing, but recent findings suggest that can also have beneficial physiological functions *in vivo* in mammals. To test this hypothesis, we transiently switched on *in situ* ROS production in mouse skin. This process activated cell proliferation in the tissue and, interestingly, in the bulge region of the hair follicle, a major reservoir of epidermal stem cells, promoting hair growth as well as stimulating tissue repair after severe burn injury. We further show that these effects were associated with a transient Src kinase phosphorylation at Tyr416 and with a strong transcriptional activation of the prolactin family 2 subfamily c of growth factors. Our results point to potentially relevant modes of skin homeostasis regulation and demonstrate that a local and transient ROS production can regulate stem cell and tissue function in the whole organism.

INTRODUCTION

The skin is the largest organ in mammals, consisting of three layers, epidermis, dermis and hypodermis, with associated appendages, including hair follicles, sebaceous and sweat glands. The biology of epidermal stem cells in the skin is well known (Blanpain and Fuchs, 2009; Baker and Murray, 2012). In particular, the pilo-sebaceous unit (hair follicle and associated glands) and the hair follicle growth cycle constitute a very well characterized model to study the functional regulation of skin stem cells. The hair follicle is a complex mini-organ that invaginates from epidermal sheets of the skin into the dermis (Muller-Rover et al, 2001; Baker and Murray, 2012; Gilhar et al, 2012). Hair production is the result of a cyclic activity of the hair follicle alternating three sequential phases: anagen (growth), catagen (cessation and regression) and telogen (rest). The hair follicle is divided in two main regions depending on size variation rates through the hair cycle: permanent and cyclic regions. The upper permanent region, composed by the infundibulum, associated glands and the bulge, a major reservoir of hair follicle stem cells, regulates the activity of the dermal papilla in the cyclic region (Ramos et al, 2013). Activation of dermal papilla cells during the anagen phase promotes extensive cell proliferation and differentiation in the cyclic region, ultimately resulting in the formation and growing of the hair shaft. Skin components are constantly renewed by a stock of multipotent epidermal stem cells, located in the bulge region of the hair follicle and in the basal layer of the inter-follicular epithelium (Blanpain and Fuchs, 2009; Baker and Murray, 2012).

Important and well known molecular mechanisms, including Wnt/β-catenin, BMP/Tgfβ/Smad, PI3K/Akt and ERK/MAPK signalling pathways (Baker and Murray, 2012; Lopez-Pajares et al, 2013; Ramos et al, 2013), have key roles in the regulation of different aspects of skin stem cell and hair follicle function. However, skin homeostasis and the hair follicle cycle are extremely complex and multifactorial processes. Many of the interplaying mechanism that govern and/or modulate the functional output of these processes are not well characterized. In particular, the potential physiological role of reactive oxygen species (ROS) in the skin is largely unknown.

The generation of reactive oxygen species (ROS) as by-products of essential and efficient metabolic reactions, such as cellular respiration or oxidase activity, is an inevitable biochemical side-effect that can be extremely harmful for cell viability. The oxidative stress induced by the undesirable intracellular accumulation of ROS is a major cause of cell and tissue toxicity and it is associated with several human diseases, including neurodegenerative (Parkinson's, Alzheimer's and Huntington's diseases), psychiatric (schizophrenia and bipolar disorder) and cardiovascular (stroke and myocardial infarction) disorders (Pieczenik and Neustadt, 2007; Valko et al, 2007). ROS are also implicated in sickle cell disease and the fragile X and chronic fatigue syndromes (el Bekay et al, 2007; Pieczenik and Neustadt, 2007). The so called oxidative stress or free radical theory of aging proposes a causal link between gradual, time-dependent ROS production during the whole lifetime and aging of the organism, a controversial theory that remains the subject of intense debate (Perez et al, 2009; Speakman and Selman, 2011).

Aerobic organisms have evolved powerful mechanisms to manage excess ROS production and are able to efficiently detoxify superoxide anions, hydroxyl radicals, hydrogen peroxide and organic hydroperoxides into harmless H_2O and O_2. These mechanisms are exemplified by the superoxide dismutase, catalase, and glutathione peroxidase enzymatic systems (Machlin and Bendich, 1987; Fernandez and Videla, 1996; Mates and Sanchez-Jimenez, 1999). Interestingly, in the course of evolution, eukaryotic organisms have also developed systems to use ROS production for their own benefit. An example is the phagocyte, an essential cell player of the mammalian immune system that can produce radical oxygen and nitrogen species in a tightly controlled way to kill target pathogens (Klebanoff et al, 1983; Bylund et al, 2010).

Accumulated evidence suggests that eukaryotic cells can also actively promote the production of small amounts of ROS as part of signalling pathways that regulate cell survival and proliferation (Droge, 2002, Chiarugi and Cirri, 2003, Bartosz, 2009, Sena and Chandel, 2012). Furthermore, it has been reported that exogenous ROS can regulate stem cell function in *in vitro* systems (Le Belle et al, 2010). An abnormal ROS production has been also linked to the deregulation of intestinal stem cell proliferation that occurs during colorectal

cancer initiation (Myant et al, 2013). These observations imply the existence of widespread ROS-dependent mechanisms for the regulation of cell function and tissue homeostasis. Here we have used the skin and the well characterized epidermal stem cell niche located in the bulge region of the mouse hair follicle as a working model to provide a proof-of-concept for the hypothesis that a transient modulation of *in situ* ROS levels can regulate skin homeostasis and stem cell function in a whole organism.

RESULTS

-Photodynamic treatment of mouse skin with mALA and red light induces a transient *in situ* ROS production in the tissue.

To this end we first developed a reproducible method to promote a controlled and transient increase of ROS in the skin. High levels of intracellular ROS can be generated by a combination of light of an adequate wavelength and a photosensitizer (PS) in the presence of O_2 (Juarranz et al, 2008). The resulting photodynamic effect (Figure S1a) is widely used as a powerful cell killing method in clinical practice (photodynamic therapy) for the treatment of several skin diseases, including cancer and infections. At present, 5-aminolevulinic acid (ALA) or its methyl derivative (mALA) in combination with red light is the most widely used photodynamic therapy in the clinic. These compounds are not PS *per se*, but function as precursors of the endogenous PS Protoporphyrin IX (PpIX) (Figure S1b) (Juarranz et al, 2008).

We have previously demonstrated that mALA can be used to photo-generate tightly controlled low levels of intracellular ROS that are able to stimulate cell proliferation instead of cell death in cultured immortalized keratinocytes (Blazquez-Castro et al, 2012). Here, we have adapted this approach to mouse skin *in vivo*. We have evaluated irradiation doses from 2 to 10 J/cm^2 and a fixed mALA concentration (25 mg Metvix®, mALA 160 mg/g cream). We found that topical application of mALA on mouse dorsal skin promoted an extensive production and accumulation of PpIX in the tissue, as revealed by the characteristic reddish fluorescence of this compound under blue light (407 nm) excitation (Figure 1a). As expected, mALA-dependent PpIX accumulation in the

skin followed by 2.5 J/cm^2 irradiation with red light (636 nm) to complete the photodynamic treatment (mALA+Light) resulted in a significant increase of *in situ* ROS levels in the tissue (Figure 1b). A time-course analysis showed that relative ROS production was transient, returning to initial levels 100 min after irradiation (Figure 1b). To gain further detail on the distribution of generated ROS in the tissue we used the manageable mouse tail skin epithelium. Accordingly, experimental treatments and the localization of PpIX and ROS were evaluated *ex vivo* in whole pieces of the tissue. We established that incubation with mALA resulted in a significant accumulation of PpIX in the hair follicle (Figure 1c), followed by a notable production of ROS after 10 J/cm^2 of red light irradiation (mALA+Light) that was detected to some degree all over the epidermis, including IFE, infundibulum and sebaceous glands (Figure 1d). Notably, ROS signal rapidly disappeared or declined in most tissue locations, persisting for longer times in bulge cells (Figure 1d), which is the main niche or reservoir of epidermal stem cells in the skin. As these experiments were performed *ex vivo* to determine ROS localization, the time course of ROS production is not comparable to that observed *in vivo* in back skin. However, these results corroborate the transient nature of ROS production in the skin induced by our experimental approach, as well as the remarkable incidence on the bulge stem cell niche.

To rule out deleterious effects of our protocol on cell and tissue viability we used different approaches. We analysed the formation of phosphorylated histone H2AX (pH2AX; also known as gammaH2AX) foci on the chromatin fibre that are associated with severe DNA damage (Yuan et al, 2010). No significant differences were observed in the number and distribution of pH2AX positive cells in the skin in samples irradiated with red light after mALA application, as compared to light control samples (Figure S2a). In sharp contrast, a strong increase in the number of cells showing pH2AX foci was observed in UV irradiated skin (Figure S2a). In the same way, we found that mALA+Light was unable to induce a noticeable increase in the number of apoptotic cells in the interfollicular epithelium or in the hair follicle (Figure S2b). Finally, we also evaluated whether our protocol could alter the incidence of skin tumour formation. We performed two series of experiments involving a single

mALA+Light (n=5) or a dual treatment in a 15 day period (n=3). In both cases, our results indicated that the mALA+Light treatment was completely safe and had no detectable or significant capacity to induce tumours in long-term experiments (up to 18 months).

-Switching on *in situ* ROS production in the skin activates cell proliferation in epidermal and dermal layers and in the hair follicle stem cell niche.

We next investigated the potential effects of the transient ROS increase induced by mALA+Light on the function of epidermal stem cells in the bulge region of the hair follicle. To this end, we first proceeded to identify stem cells as label retaining cells (LRC) in pulse and long-chase experiments with the nucleotide analogue 5-bromo-2´-deoxyuridine (BrdU) (Braun et al, 2003). We quantified the number of LRC in the bulge region of hair follicles at 7 weeks after birth, during which time hair follicles are in a refractory telogen or resting phase of the growth cycle and are insensitive to stimulatory signals (Muller-Rover et al, 2001). We found that the transient *in situ* ROS production induced by mALA+Light activated the proliferation of bulge stem cells, promoting a significant increase in the number of BrdU labelled cells, that was first detected in the skin 2 days after the treatment (Figure 2a). This was associated with a strong and parallel increase in the number of dividing (Ki67 positive) cells in the bulge region (Figure 2b), indicating a proliferative response of the hair follicle stem cell niche. The number of BrdU labelled cells reverted to normal levels, as compared to control animals, 6 days after the treatment (Figure 2a), indicating the transient nature of the biochemical stimulus. These results were confirmed using a transgenic murine model in which GFP is expressed under the control of the *keratin1- 15* promoter, a molecular marker of hair follicle epidermal stem cells (Morris et al, 2004). We found a significant increase of GFP positive cells in the bulge region of the hair follicle 2 days after mALA+Light that returned to normal levels 6 days after the treatment (Figure S3).

We also observed that mALA+Light promoted a transient increase in the number of proliferating cells in the epidermal and dermal layers of the skin starting 2 days after the treatment and returning to normal levels by day 6

(Figure 2c; Figure S4a). This proliferative pulse was associated with a transient epidermal hyperplasia and a significant increase of dermal cellularity 2 days after treatment that disappeared by day 6 (Figure 2c; Figure S5c). A strong cornification was also observed in treated skin regions (Figure 2c), suggesting an overall acceleration of tissue turnover rate. These processes were not associated with histopathological features of inflammation or to the induction of molecular skin inflammation markers, like myeloperoxidase (MPO) (Figure 2c; Figures S4b, S5c). As a whole, these results are in agreement with our previous report in cultured keratinocytes (Blazquez-Castro et al, 2012) and indicate that a transient production of ROS in the skin promotes a transient proliferative response in the tissue that can activate the epidermal stem cell niche.

-Switching on *in situ* ROS production in the skin stimulates hair growth and accelerates burn healing.

We reasoned that the effect of mALA+Light on cell proliferation in the skin and, particularly, on stem cells contained in the hair follicle bulge region should produce a physiological response in the target tissue. Supporting this concept, we observed that mALA+Light strongly promoted hair growth after shaving stimulation during the refractory telogen phase (Figure 3a; Figure S5a). Importantly, the use of anti-oxidant compounds like ascorbic acid (AA) and N-acetylcysteine (NAC) abolished the differences in hair follicle growth rates induced by mALA+Light with respect to Light control skin (Figure 3a, b; Figure S5a). In agreement with this observation, anti-oxidant treatment significantly inhibited the production of ROS (Figure 3a, c) and the activation of cell proliferation (Figure 3d) induced by mALA+Light in the tissue. It is to note that, since we have observed inter-individual variations in the timing of hair growth in a day-range after the shaving stimulus, the comparisons between treated and control skin to quantify the mALA- phototreatment (mALA-PT) output were always established between different skin regions in the same mouse.

Morphological features and Lef1 expression in the hair germ indicated that anagen entry occurred about 6 days after treatments in mALA+Light treated skin but not in the correlative Light treated skin controls or in non-treated skin (normal anagen, NA) showing spontaneous anagen entry (Figure 3e). As

expected, anagen entry was also observed in Light controls and non-treated skin about 10 days after treatments as a consequence of shaving stimulation, showing Lef1 expression and cell proliferation in the hair germ and dermal papilla (Figure 3e, f). However, mALA+Light treated skin consistently showed larger hair follicles with extensive cell proliferation at equivalent time points (Figure 3e, f). As a whole, these results indicate that a controlled and transient production of ROS in the skin can bypass the strong inhibitory signalling that occurs at refractory telogen of the hair follicle cycle, forcing the premature entry into the anagen growth phase.

These results prompted us to investigate the ability of the transient ROS production to stimulate the regenerative potential of the skin. To this end, we performed a series of burn healing experiments. As shown in Figure 4, mALA+Light significantly accelerated the healing process after 2nd-degree burn injuries in the skin. Remarkably, this regenerative effect was associated with extensive cell proliferation in the bulge region of hair follicles adjacent to the burned area (Figure 4d), indicating the activation of this stem cell niche. Taken together, these results suggest that the activation of skin proliferation and of the hair follicle stem cell niche by a transient ROS production is a molecular signal able to stimulate different homeostatic programs in the skin, including hair growth and tissue regeneration.

-Switching on *in situ* ROS production in the skin promotes a transient activating phosphorylation of cSrc kinase

We next sought to investigate the molecular mechanisms underlying the stimulation of skin induced by mALA+Light treatments that, as demonstrated above, results in a transient proliferative wave 2 days after the treatment returning to normal levels by day 6. We focused on this time period and on signalling pathways known to have key roles in the activation of epidermal stem cell function and hair follicle growth, including Wnt/β-catenin, MAPK and PI3K/Akt signalling pathways. Interestingly, no changes in expression levels of either β-catenin or a metabolically stable, constitutively active form of this protein were detected after mALA+Light treatment (Figure 5a). Accordingly, no significant changes in the distribution of β-catenin were observed in

mALA+Light treated skin as compared to control samples, in both cases showing a major localization at the cell membrane and no nuclear translocation (Figure S6a), a key indicator of β-catenin dependent transcriptional activation. As described above (Fig. 3e) and as expected, Lef1 expression was found in hair follicles since day 6 and was remarkable on advanced anagen, around 10 days after mALA-PT. In a similar way, no changes of phosphorylation at critical Thr/Tyr residues in different mitogen-activated protein kinases (MAPK) including JNK, p38 and ERK1/2, which are key indicators of signalling pathway activation, were observed after mALA+Light (Figure S6b). By contrast, a significant increase in phosphorylated Akt, similar to the increase observed in a neurosphere model (Le Belle et al, 2010), and a strong phosphorylation of Src kinase at Tyr416 were transiently detected 2 days after mALA+Light (Figure 5a). Interestingly, Src protein showed an increased accumulation in the epidermis of mALA+Light skin samples 2 days after treatment that disappeared at day 6 (Figure 5b). These results are consistent with our previous observations indicating a role for Src in the ROS-dependent induction of cell proliferation in human keratinocytes (Blazquez-Castro et al, 2012).

-Switching on *in situ* ROS production in the skin induces a transient transcriptional activation of prolactin family 2 subfamily c members.

To get a deeper insight into the molecular mechanism underlying the ROS-dependent, Src-driven activation of the epidermal stem cell niche we performed a series of large-scale microarray analyses of mRNA expression, both in back and tail epidermis after mALA+Light as compared to control samples (GEO accession number GSE55135). Several genes showed significant transcriptional alterations 2 days after mALA+Light that were similarly modulated in tail and back epidermis (Table 1). It is to note that this large-scale analysis showed that mALA-PT was not associated with transcriptional profiles of inflammation or injury response. The transcriptional profiles of genes of interest were validated in all cases by qRT-PCR in dorsal skin at both 2 or 6 days after mALA+Light (Figure 5c), revealing that the majority of genes transcriptionally altered at 2 days returned to normal expression levels 6 days after the treatment. In agreement with our previous observations, targets of Wnt/β-catenin signalling in the skin, such as Jag1, Ovol1 and Axin2, were

transcriptionally repressed 2 days after mALA+Light (Figure 5c). Interestingly, the strongest transient transcriptional activation induced by mALA+Light was observed for members of the prolactin family 2 subfamily c of growth factors. In particular, *Prl2c3*, also known as *proliferin-2*, showed a marked transient activation 2 days after switching on ROS production by mALA+Light (Table 1; Figure 5c). More surprisingly, we found a significantly increased expression of Prl2c3 protein in the skin associated with a strong nuclear localization in the hyperplastic interfollicular epidermis (Figure 5d).

DISCUSSION

Here we have shown that switching on *in situ* ROS production can regulate functional responses in a tissue through the stimulation of cell proliferation and of a stem cell niche. Our results are in agreement with recent reports showing a role for ROS during the stimulation of neural stem cells *in vitro* in a neurosphere model (Le Belle et al, 2010) and in the deregulation of intestinal stem cell proliferation that occurs during colorectal cancer initiation (Myant et al, 2013). In these studies an exogenous and/or continuous ROS supply or a systemic ROS depletion is used to evaluate a specific effect on a tissue or biological systems. As a complement to these studies, our experimental approach implies a local and transient activation of endogenous ROS production using the molecular machinery of the tissue. In this sense our results are in close consonance with the observation that a transient ROS production occurs during tail regeneration in *Xenopus* tadpoles (Love et al, 2013). In this report it is shown that activation of a regenerative signal, i. e. cutting the tadpole, is accompanied by a transient production of ROS. Here we demonstrate that a transient ROS switch on activates a regenerative signal. It has also been reported that the mitochondrial transcription factor A (TFAM) is required for normal hair follicle development and *in vitro* keratinocyte differentiation (Hamanaka et al, 2013), suggesting indirectly that mitochondrial ROS can have an important role in the regulation of skin function. Here we directly demonstrate that a transient generation of ROS in the mouse skin activates the hair follicle stem cell population, promoting hair growth in the refractory telogen phase and accelerating burn healing. In this context, it would be interesting to evaluate the clinical potential of a transient ROS production *in situ* in the skin to stimulate tissue homeostasis, for example,

to improve the healing process of small burns and chronic wounds or to activate hair growth or prevent hair loss in certain types of alopecia.

We have found that switching on *in situ* ROS production by mALA-PT promotes a transient proliferative pulse in the tissue, including bulge cells, 2 days after the treatment. This proliferative burst results in extensive anagen development of hair follicles by days 8-10, showing extensive cell proliferation and Lef1 expression particularly in the hair germ, and subsequent hair growth by days 12-19 after mALA-PT. At day 2 most hair follicles are in telogen and, consequently, no evidence of β-catenin accumulation or transcriptional activation of Wnt/β-catenin signaling is observed. However, a significant activating phosphorylation of cSrc occurs at this time point. This result is particularly interesting, since no significant roles are usually assigned to Src kinase in relation to the regulation of skin stem cell function and/or the hair follicle growth cycle. However, it has been reported that Src protein expression and activity are regulated during normal hair follicle cycle (Serrels et al, 2009). In the same context, the molecular mechanisms regulating Src kinase activity by ROS in cultured cells are well characterized (Giannoni et al, 2010). These observations suggest that Src activity, independently or in combination with a controlled ROS production, can be an important partner in the skin signalling network, which merits further investigation. In this context, we hypothesize that mALA-PT induces 2 days after treatment an initial, cSrc-dependent, proliferative wave in the skin able to activate hair follicle stem cell niches. This activation results in standard, Lef1 dependent, anagen entry around 6 days after treatments.

We have further shown that a transient ROS production switching on in the skin promotes a strong and unexpected transcriptional activation of prolactin family 2 subfamily c gene members, particularly *Prl2c3*. Surprisingly, we found that Prl2c3 was significantly translocated to the nucleus in most cell layers in the hyperplastic epithelium after mALA+Light, suggesting that this hormone-like protein can have nuclear functions. Interestingly, it has been reported that this mitogen is expressed in the hair follicle anagen growth phase (Fassett and Nilsen-Hamilton, 2001) and facilitates the expansion of hematopoietic stem cells *ex vivo* (Choong et al, 2003). The role of Prlc3 in the skin is currently under

investigation. In this context, the procedure presented here to transiently activate endogenous ROS production in the skin has proved to be an efficient tool not only to suggest a physiological role for ROS *in vivo* but also to identify new signalling pathways and factors potentially implicated in the regulation of skin homeostasis.

MATERIALS AND METHODS

Animals

Seven-week-aged C57BL/6 mice, including the strain B6.Cg-Tg(Krt1-15-EGFP)2Cot/J (Morris et al, 2004), were used. When possible, littermates were included in each experiment and comparisons were done between animals of the same sex. Both males and females were used in experiments using tail skin. Only females were used in experiments performed in back skin. All animal husbandry and experimental procedures were conducted in compliance with 2010/63/UE European guideline or approved by the Subcommittee on Research Animal Care (IACUC) of Massachusetts General Hospital (Boston, MA), in accordance with the guidelines of the National Institutes of Health (NIH).

Identification of Label Retaining Cells (LRC) in tail skin epithelium

Long-term 5-bromo-2'-deoxyuridine (BrdU; Sigma-Aldrich) label retaining cells (LRC) were generated and characterized as previously described (Braun et al, 2003). Briefly, ten-day-old mice were injected intraperitoneally (i. p.) once a day during 4 consecutive days with 50 mg/kg bodyweight BrdU dissolved in PBS. After the labelling phase, mice were allowed to grow until the age of 7 weeks before any treatment. To prepare whole-mounts of tail epidermis, tails were clipped, skin was peeled from tails and incubated in 5 mM EDTA in PBS 4 h at 37 ºC. Intact sheets of epidermis were separated from the dermis using forceps and fixed in 4% formaldehyde in PBS.

Burning procedure

For induction of burn injuries, mice were anesthetized and shaved. A brass bar (1 cm in cross-section) pre-heated (~95 ºC) by immersing in boiling water was applied on the dorsal surface of each mouse and maintained in contact with the skin for 5 seconds. The resulted nonlethal, partial-thickness, 2nd degree burns measured approximately 1.3-cm × 1.3-cm. For the analysis of proliferating cells around the wound, animals received 2 sequential i. p. injections of 50 mg/kg bodyweight BrdU every 12 hours, starting 4 h after mALA-PT.

Photodynamic treatments

All experiments were performed during the refractory telogen phase of the hair follicle growth cycle (7-week-old mice). For photodynamic treatments, mALA as topical cream (Metvix®, Galderma) was used. For tail skin experiments, Metvix® was applied directly on the skin. For back skin treatments, animals were completely shaved with a hair clipper and depilatory cream (Veet®) and washed with PBS. We applied 25 mg of Metvix® covering the area of interest. After 2.5 h of incubation in darkness, animals were anesthetized and the accumulation of PpIX was evaluated *in situ* by measuring the characteristic red fluorescence under 407 nm blue light excitation. To conduct the photodynamic treatments (mALA+Light), a red light (636 nm) emission was subsequently applied on the dorsal surface of the tissue to a total dose of 2.5- 10 J/cm^2, using a LED lamp (Aktilite®). Light control animals received only red light, while Dark control animals received only mALA and they were kept in dark at least 48 h after the

treatment. For inhibitory experiments using ascorbic acid (AA, from Sigma), two doses of 100 mg/ml AA in 50% ethanol spaced 30 min were topically applied on the skin between the application of mALA and red light irradiation. For the alternative experiments using N-acetylcysteine (NAC, from Sigma), a solution containing 20 mg/ml NAC in PBS was i.p. inoculated daily during 5 days at a dose of 100 mg/kg bodyweight, until the day that mALA-PT was applied. Photodynamic treatments on burned skin were performed 24 h after the burning procedure. In all cases, the % of animals showing hair growth acceleration in treated back skin regions as compared to control regions in the same animal was evaluated. An animal showing hair growth acceleration was defined as an animal showing full hair growth all along the treated region, typically by days 12-19 after shaving, but only limited or no hair growth in the control region.

Monitoring ROS production

ROS production in tail skin was evaluated *ex vivo* using hydroethidine (Sigma-Aldrich), which reacts with ROS to produce fluorescent dye hET. Samples were incubated at 37 ºC for 3 h in a solution with 5 mM EDTA in PBS, containing 2 mM mALA in the case of treated samples. Hydroethidine was added to a final concentration of 3.2 µM. After 1 h, the skin was irradiated with 10 J/cm^2 of 636 nm light and fixed.

For *in vivo* detection of ROS produced in back skin during photodynamic treatment, the ROS sensitive DHF-DA (Sigma-Aldrich) was used. In order to assess the inhibitory effect of AA, two independent groups of animals were established for each time point for normalizing the obtained signal (mALA+Light/Light) with respect to AA-animals. After dorsal skin shaving and PT treatment application as previously described (Metvix® 2.5 h in dark followed by the irradiation with 2.5 J/cm^2 of 636 nm light), 1 mg/ml DHF-DA in 50% ethanol was topically applied on the tissue at different time points after the irradiation (5, 20 and 100 min). ROS levels generated in the skin were determined 45 min after the application of DHF-DA in all cases, using an IVIS® Lumina 2 imaging system (Xenogen), by measuring the fluorescent signal emitted by the fluorescein produced through the oxidation of DHF-DA. The filters setting were 445-490 nm for the excitation and 515-575 nm for the emission.

Immunological and histological methods

Primary antibodies used were FITC-conjugated mouse monoclonal anti BrdU (Roche); rabbit monoclonal antibodies against Src, Phospho-Src (Tyr416), AKT, Phospho-AKT (Ser473), p38 MAPK, Phospho-p38 MAPK (Thr180/Tyr182), p44/42 MAPK, Phospho-p44/42 MAPK (Thr202/Tyr204), Phospho SAPK/JNK (Thr183/Tyr185) and gammaH2AX (Ser 139) and Lef1 (all from Cell Signaling Technologies); rabbit monoclonal anti Ki67 (Neo Markers); rabbit polyclonal anti Src (Abcam); mouse monoclonal anti β-catenin (BD); mouse monoclonal anti Active-β-catenin (Millipore); goat polyclonal anti-Proliferin 2 (Prl2c3) and anti-MPO (both from Santa Cruz Biotechnology); mouse monoclonal antibodies against PCNA (Calbiochem), tubulin and BrdU (both from Sigma).

For BrdU-FITC immunostaining in tail skin epithelium whole-mounts, fixed epidermal pieces were sequentially treated with 1 N HCl 45 min at 37 ºC, Tris-borate-EDTA 5 min at RT and washed abundantly with distilled water. Permeabilization and blocking were carried out by incubation with PTG buffer (PBS containing 0.5% Triton X-100 and 0.2% gelatin) for 30 min at RT. Then, samples were incubated with the FITC-conjugated primary antibody against BrdU (Roche) diluted 1:50 in PBS, overnight at 37 ºC. For fluorescence immunostaining of pH2AX, positive control samples were obtained from animals exposed to a total dose of 7.44 J/cm^2 of UVB light, using a lamp with a 312 nm emission peak (Philips TL UV). Apoptosis was detected in whole-mounts using the TUNEL detection kit (Roche) following the instructions of the manufacturer. Images were obtained in Leica TCS SP2 AOBS spectral confocal microscope and processed using FIJI software.

For immunohistochemical staining, hydrated paraffin samples were treated with tripsin (Thermo Scientific) 30 min at 37 ºC before incubating overnight with primary antibodies and revealed using the Envision Flex/HRP (Dako) secondary antibodies cocktail and DAB kit (Vector Laboratories).

For immunobloting, skin samples were homogenized at 4 ºC in cold NT lysis buffer (50 mM Tris-HCl, pH 7.4, 100 mM NaCl, 5 mM $MgCl_2$, 5 mM $CaCl_2$, 1% NP-40, 1% Triton X-100, 2 mM, PMSF, 20 µg/ml aprotinin and 1 mM sodium orthovanadate).

RNA extraction and gene expression analysis

RNA was isolated form back skin and back and tail epidermis with TriPure™ Isolation Reagent (Roche) and RNeasy Mini kit (QIAGEN). Gene expression signatures were characterized using standardized mouse global mRNA expression arrays (Agilent Technologies; Agilent.SingleColor.14868). Gene expression analysis included pool samples (n=3) obtained 2 days after the treatment. Pools prepared from both back and tail epidermis were independently analysed. Large-scale gene expression results were validated by real-time quantitative RT-PCR (qRT-PCR) in back skin samples. Primer sequences are available upon request.

Statistical analysis

Quantifications of LRC and Krt1-15-GFP expression in the bulge region were performed on confocal images (30 hair follicles/animal, 3 animals/group). BrdU positive cells were quantified in the 3 hair follicles closest to the burned area in 3 different animals per condition. Comparisons between groups were performed by Student's t test using the SPSS 15.0 software. Skin thickness was measured in 10 different regions of interfollicular epidermis per mouse including 3 animals per condition.

In vivo ROS production detected with the IVIS® Lumina 2 was quantified using FIJI software. The relative DHF-DA Integrated density was calculated for each mouse as the ratio of the integrated density obtained in mALA-treated skin related to Light control area. For the statistical comparison, the integrated density was normalized calculating the ratio (vehicle/AA) for all possible pairs

between AA and vehicle-treated animals for each time point. The average and standard error (SE) were represented and means of different time points were compared using ANOVA.

For statistical analyses of gene expression data, an unpaired t-test was applied, setting $p \leq 0.05$ and fold change ≥ 2.0 as limits for significance. qRT-PCR data were analysed by a comparative C_T method, using 18S rRNA expression as internal control. Gene expression fold changes were represented as the ratio between means of $2^{-\Delta Ct}$ values of mALA+Light and Light control groups mean values. Differentially expressed genes were selected based on the Student's t test comparison of means of $2^{-\Delta Ct}$ values between both groups.

For quantification of burn assays, day-to-day digital images were analysed. The unhealed area was quantified using FIJI software. The area-under-the-curve was calculated separately for each mouse and means were compared by the Student's t test.

CONFLICT OF INTEREST

The authors declare no competing financial interest. Clinical and commercial applications of the experimental procedures described in this work have been registered by a CSIC-UAM patent.

ACKNOWLEDGEMENTS

JE was supported by Spanish MINECO grants SAF11-23493 and RTC-2014-2626-1 and Comunidad Autónoma de Madrid grant SkinModel CAM S10/BMD-2359. DV and MRH were supported by US NIH grant R01AI050875. AJ was supported by Spanish MINECO grant FIS PI12/01253 and CAM S10/BMD-2359. JCS was supported by Spanish MCINN grant CTQ2010-20870-C03-03. EC and MIC were supported by Spanish MECD-FPU and UAM-FPI fellowships, respectively. We thank to Dr. Colin Jahoda for the kind review of this manuscript. We thank to biocellavi.com for assistance in the preparation of figures.

REFERENCES

Baker RE, and Murray PJ (2012). Understanding hair follicle cycling: a systems approach. *Curr Opin Genet Dev* 22:607-12.

Bartosz G (2009). Reactive oxygen species: destroyers or messengers? *Biochem Pharmacol* 77:1303-15.

Blanpain C, and Fuchs E (2009). Epidermal homeostasis: a balancing act of stem cells in the skin. *Nat Rev Mol Cell Biol* 10:207-17.

Blazquez-Castro A, Carrasco E, Calvo MI, et al (2012). Protoporphyrin IX-dependent photodynamic production of endogenous ROS stimulates cell proliferation. *Eur J Cell Biol* 91:216-23.

Braun KM, Niemann C, Jensen UB, et al (2003). Manipulation of stem cell proliferation and lineage commitment: visualisation of label-retaining cells in wholemounts of mouse epidermis. *Development* 130:5241-55.

Bylund J, Brown KL, Movitz C, et al (2010). Intracellular generation of superoxide by the phagocyte NADPH oxidase: how, where, and what for? *Free Radic Biol Med* 49:1834-45.

Chiarugi P, and Cirri P (2003). Redox regulation of protein tyrosine phosphatases during receptor tyrosine kinase signal transduction. *Trends Biochem Sci* 28:509-14.

Choong ML, Tan AC, Luo B, et al (2003). A novel role for proliferin-2 in the ex vivo expansion of hematopoietic stem cells. *FEBS Lett* 550:155-62.

Droge W (2002). Free radicals in the physiological control of cell function. *Physiol Rev* 82:47-95.

el Bekay R, Romero-Zerbo Y, Decara J, et al (2007). Enhanced markers of oxidative stress, altered antioxidants and NADPH-oxidase activation in brains from Fragile X mental retardation 1-deficient mice, a pathological model for Fragile X syndrome. *Eur J Neurosci* 26:3169-80.

Fassett JT, and Nilsen-Hamilton M (2001). Mrp3, a mitogen-regulated protein/proliferin gene expressed in wound healing and in hair follicles. *Endocrinology* 142:2129-37.

Fernandez V, and Videla LA (1996). Biochemical aspects of cellular antioxidant systems. *Biol Res* 29:177-82.

Giannoni E, Taddei ML, and Chiarugi P (2010). Src redox regulation: again in the front line. *Free Radic Biol Med* 49:516-27.

Gilhar A, Etzioni A, and Paus R (2012). Alopecia areata. *N Engl J Med* 366:1515-25.

Hamanaka RB, Glasauer A, Hoover P, et al (2013). Mitochondrial reactive oxygen species promote epidermal differentiation and hair follicle development. *Sci Signal* 6:ra8.

Juarranz A, Jaen P, Sanz-Rodriguez F, et al (2008). Photodynamic therapy of cancer. Basic principles and applications. *Clin Transl Oncol* 10:148-54.

Klebanoff SJ, Locksley RM, Jong EC, et al (1983). Oxidative response of phagocytes to parasite invasion. *Ciba Found Symp* 99:92-112.

Le Belle JE, Orozco NM, Paucar AA, et al (2010). Proliferative neural stem cells have high endogenous ROS levels that regulate self-renewal and neurogenesis in a PI3K/Akt-dependant manner. *Cell Stem Cell* 8:59-71.

Lopez-Pajares V, Yan K, Zarnegar BJ, et al (2013). Genetic pathways in disorders of epidermal differentiation. *Trends Genet* 29:31-40.

Love NR, Chen Y, Ishibashi S, et al (2013). Amputation-induced reactive oxygen species are required for successful Xenopus tadpole tail regeneration. *Nat Cell Biol* 15:222-8.

Machlin LJ, and Bendich A (1987). Free radical tissue damage: protective role of antioxidant nutrients. *Faseb J* 1:441-5.

Mates JM, and Sanchez-Jimenez F (1999). Antioxidant enzymes and their implications in pathophysiologic processes. *Front Biosci* 4:D339-45.

Morris RJ, Liu Y, Marles L, et al (2004). Capturing and profiling adult hair follicle stem cells. *Nat Biotechnol* 22:411-7.

Muller-Rover S, Handjiski B, van der Veen C, et al (2001). A comprehensive guide for the accurate classification of murine hair follicles in distinct hair cycle stages. *J Invest Dermatol* 117:3-15.

Myant KB, Cammareri P, McGhee EJ, et al (2013). ROS production and NF-kappaB activation triggered by RAC1 facilitate WNT-driven intestinal stem cell proliferation and colorectal cancer initiation. *Cell Stem Cell* 12:761-73.

Perez VI, Bokov A, Van Remmen H, et al (2009). Is the oxidative stress theory of aging dead? *Biochim Biophys Acta* 1790:1005-14.

Pieczenik SR, and Neustadt J (2007). Mitochondrial dysfunction and molecular pathways of disease. *Exp Mol Pathol* 83:84-92.

Ramos R, Guerrero-Juarez CF, and Plikus MV (2013). Hair follicle signaling networks: a dermal papilla-centric approach. *J Invest Dermatol* 133:2306-8.

Sena LA, and Chandel NS (2012). Physiological roles of mitochondrial reactive oxygen species. *Mol Cell* 48:158-67.

Serrels B, Serrels A, Mason SM, et al (2009). A novel Src kinase inhibitor reduces tumour formation in a skin carcinogenesis model. *Carcinogenesis* 30:249-57.

Shao L, Li H, Pazhanisamy SK, et al (2011). Reactive oxygen species and hematopoietic stem cell senescence. Int J Hematol 94: 24-32

Speakman JR, and Selman C (2011). The free-radical damage theory: Accumulating evidence against a simple link of oxidative stress to ageing and lifespan. *Bioessays* 33:255-9.

Valko M, Leibfritz D, Moncol J, et al (2007). Free radicals and antioxidants in normal physiological functions and human disease. *Int J Biochem Cell Biol* 39:44-84.

Yuan J, Adamski R, and Chen J (2010). Focus on histone variant H2AX: to be or not to be. *FEBS Lett* 584:3717-24.

TABLE LEGENDS

Table 1. Genes significantly up- or down-regulated 2 days after mALA-PT in both back and tail epidermis. The expression ratios obtained by microarray analysis are referred to fold changes of mRNA expression in mALA+Light as compared to control samples. Associated functions were extracted from UniProt KB. TF: transcription factor.

FIGURE LEGENDS

Figure 1. Photodynamic treatment with mALA and red light induces a transient production of ROS in the skin. a) Accumulation of endogenous PpIX after mALA topic treatment in back skin. The left side in the same animal was used as control. b) Left panel: PpIX-dependent ROS (mALA+Light) production monitored by DHF-DA. Right panel: time-course analysis of relative ROS production in back skin; the relative integrated density of DHF-DA fluorescent emission of mALA+Light versus Light regions in each animal was quantified at different times after irradiation and normalized as described in methodology. The mean +/- SE was represented (n=4 for each time point). c) Localization of PpIX in tail skin (fluorescence microscopy images). d) ROS production in tail skin after mALA+Light as revealed by hET showing an increased and sustained accumulation in the bulge region of the hair follicle. Representative confocal microscopy images (maximum projections) are shown. Bars: 100 µm.

Figure 2. Switching on *in situ* ROS production in the skin activates stem cell proliferation in the hair follicle niche and promotes a transient proliferation of epidermal and dermal cells. a) BrdU label retaining cells (LRC) quantification in the hair follicle bulge region. The mean + SE (n=4) is represented. b) Immunological detection of the Ki67 proliferation marker in the hair follicle bulge region. c) Dorsal skin histological sections stained for inmunohistochemical detection of Ki67 (left panels) or with Masson´s trichrome (middle panels) showing transient effects in the skin induced by mALA+Light treatments, including cell proliferation, hyperplasia in the epidermis (vertical bars), a significant increase in dermal cellularity (squares) and strong cornification (arrowheads). Squares indicate equivalent areas in which cell numbers were quantified. Right panels show the quantification of interfollicular epidermis (IFE) thickness and dermal cellularity in 10 histological fields. The mean + SD (n=3) is represented. In a) and b) representative confocal microscopy images (maximum projections) of tail skin whole-mounts are shown. Bars: 100 µm.

Figure 3. Switching on *in situ* ROS production in the skin stimulates hair growth. a) Top row: Induction of hair growth during the refractory telogen phase by mALA+Light (right side of dorsal skin) as compared to Light control region (left side). Bottom row: Both ROS production in the skin and the acceleration of hair growth induced by mALA+Light were inhibited by AA anti-oxidant treatment. b) Quantification of the % of animals showing accelerated hair growth in mALA-PT as compared to control region in the absence or presence

of the anti-oxidant AA (n=4 in 3 independent experiments). c) Quantification of the ROS production inhibition in dorsal skin induced by AA during mALA-PT (n=4, DHF-DA was applied 20 min after irradiation). d) Inmunohistochemical detection of the PCNA proliferation marker in dorsal skin histological sections 2 days after mALA-PT showing inhibition of cell proliferation by the anti-oxidant AA. e) Inmunolocalization of Lef1 (arrowheads) in equivalent hair follicle whole-length reconstructions generated from confocal microscopy images (maximum projections) 6 and 10 days after treatments in mALA+Light and control Light treated skin and in non-treated skin (normal anagen, NA). f) Dorsal skin histological sections stained for inmunohistochemical detection of the PCNA proliferation marker 10 days after mALA-PT showing extensive cell proliferation in different regions of growing anagen hair follicles (arrowheads). Bars: 100 µm.

Figure 4. Switching on *in situ* ROS production in the skin accelerates burn healing. a) PpIX production induced by mALA in burn injured regions in treated animals as compared to control samples. b) Burn healing evolution in mALA+Light treated and control animals. c) Time-course quantification of burned areas (left panels) showing accelerated burn healing in mALA+Light treated animals; the mean +/- SE (n=4) of unhealed area is represented. Area-under-the-curve analysis (right panels) demonstrating statistical differences between both time-course curves ($p \leq 0.06$). d) Histological images showing BrdU staining of proliferating cells in the bulge region (arrowheads) of hair follicles located in the adjacent area of the burn boundary (dotted lines) in mALA+Light as compared to control samples. Right panels: quantification of the number of proliferating cells in the 3 hair follicles closest to the burn boundary. The mean + SE (n=3) is represented. Bar: 50 µm.

Figure 5. Molecular signatures associated with a transient switching on of ROS production in the skin. a) Immunoblot analysis showing a transient phosphorylation of Src kinase in mALA+Light as compared to Light control samples in back skin. b) Transient Src kinase accumulation in the epidermis of mALA+Light samples. c) Quantitative analysis of mRNA expression levels of the indicated genes in back skin. Fold change represents relative expression in mALA+Light with respect to control samples (*** $p \leq 0.001$, ** $p \leq 0.05$, * $p \leq 0.1$). d) Increased expression and nuclear translocation of Prl2c3 2 days after mALA+Light treatments. Inserts are detailed views of the nuclear distribution of Prl2c3 in epidermal keratinocytes. b) and d) correspond to representative confocal microscopy images (maximum projections). Bars: 50 µm.

SUPPLEMENTARY FIGURE LEGENDS

Figure S1. Photodynamic production of ROS using the heme biosynthetic pathway. a) Schematic representation of photochemical reactions during typical photodynamic treatments. Upon absorption of light with the appropriate λ, a photosensitizer molecule (PS) in the ground state S_0 undergoes a transition to an excited singlet state S_1. Since any excited state is energetically less preferable than the ground state, the molecule returns to S_0 after a short period of time. Most PS have a high quantum efficiency for the transition from S_1 to the

triplet state T_1, generally characterized by a relative long lifetime. Activated PS in the excited triplet state can react with other molecules via two different pathways. Type I photochemical reaction means the transfer of electrons to adjacent molecules to form radical species; these radicals are likely to react with molecular oxygen to produce ROS, including superoxide anion ($\bullet O_2^-$), hydrogen peroxide (H_2O_2) and hydroxyl radical (•OH). Type II photochemical reaction represents the dominant process for most PS employed in PDT. During this reaction, the transfer of energy (not electrons) to molecular oxygen (whose configuration in the ground state is the triplet, $^3O_2$) drives the formation of the non-radical but highly reactive singlet oxygen ($^1O_2$). The photoproducts formed during these reactions trigger a cascade of biochemical events resulting in an oxidative stress that finally causes cell death or that can potentially stimulate cell growth. b) 5-aminolevulinic acid (ALA) is a natural precursor in the heme biosynthetic pathway, which involves both mitochondrial and cytosolic cellular compartments. The ALA synthase enzyme activity is regulated by a negative feedback control whereby free heme, the final product of this pathway, inhibits the synthesis of ALA from glycine and succinyl CoA. The administration of exogenous ALA or its derivative methyl aminolevulinate (mALA) bypasses the regulatory feedback system, so that downstream metabolites, especially Protoporphyrin IX (PpIX), are accumulated in the cell inducing photosensitization. The rate-limiting characteristics of ferrochelatase, catalyst enzyme of the iron insertion in PpIX, promote the accumulation of this endogenous PS compound.

Figure S2. Switching on *in situ* ROS production in the skin does not induce molecular markers associated with DNA damage or apoptosis. a) Immunolocalization of the pH2AX protein on tail skin samples irradiated with 312 nm light (UV), 636 nm red light (Light control) or treated with mALA+ red light (mALA+Light). Extensive formation of pH2AX nuclear foci in interfollicular epithelium cells was observed in UV treated samples but not in Light control or mALA+Light samples. b) Detection of apoptotic cells by TUNEL on tail skin in Light control samples from 15 hours to 6 days after mALA+Light. No significant differences in the number of apoptotic cells were observed after mALA+Light treatments as compared to control samples. In all cases are shown representative confocal microscopy images (maximum projections) corresponding to whole-mounts of tail skin epidermis. Bars: 50 µm.

Figure S3. Switching on *in situ* ROS production in the skin activates stem cell proliferation in the hair follicle niche. Detection and quantification of cells expressing GFP under the control of the *keratin1-15* promoter (Krt1-15-GFP), a marker of epidermal stem cells, in the bulge region of the hair follicle. Tail skin samples were obtained 2 (a) or 6 (b) days after Light and mALA+Light treatments. The integrated density of GFP expression in the bulge region from at least 30 hair follicles in three different mice was calculated as described in Materials and Methods, and the mean +/- SE is represented. Images correspond to maximum projections of confocal microscopy reconstructions from tail skin whole-mounts. Bar: 100 µm.

Figure S4. Switching on *in situ* ROS production in the skin promotes a transient proliferation of epidermal and dermal cells. Inmunohistochemical detection in dorsal skin histological sections of the PCNA proliferation marker

(a) and the Myeloperoxidase (MPO) inflammation marker (b) 1, 2 or 6 days after mALA+Light treatments. Sections of mouse lung were used as positive control for MPO expression (arrowhead). Bars: 100 µm.

Figure S5. Switching on *in situ* ROS production in the skin stimulates hair growth and promotes a transient hyperplasia in the skin. a) Representative images of a mouse shaved in left and right independent regions of dorsal skin. Left area was the Light control skin in which no mALA was applied. Right area was the mALA-treated skin, which produced PpIX. Treatments were performed in the presence or absence of the i.p. inoculated anti-oxidant NAC. Upper panels: in the absence of NAC, abundant hair growth was observed between days 14 and 19 in the mALA+Light treated dorsal skin. No traces of hair growth were observed in the Light control skin. Lower panels: in the presence of NAC, the stimulatory effect of mALA-PT on hair growth was inhibited. Right panel: quantification of the % of animals showing accelerated hair growth in mALA-PT as compared to control region in the absence (n=8 in 4 independent experiments) or presence (n=2 in 4 independent experiments) of the anti-oxidant NAC. b) Histological sections stained with Haematoxylin/Eosin of Light control or mALA+Light skin samples obtained 10 days after the treatment. Anagen hair follicles were extensively formed after mALA-PT. Bars: 100 µm. c) Histological sections stained with Haematoxylin/Eosin showing a strong hyperplasia in the epidermis 2 days after mALA-PT that completely disappeared by day 6. Lower panels are detailed views on the regions indicated in upper panels. b) and c) correspond to experiments in the absence of NAC. Bars: 20 µm.

Figure S6. Switching on *in situ* ROS production in the skin does not promote the nuclear translocation of β-catenin in epidermal cells and does not activate p38, p44/42 or JNK mitogen-activated protein kinases (MAPK) signalling pathways. a) Representative confocal microscopy images (maximum projections) showing the immunolocalization of β-catenin on back skin histological sections. A strong hyperplasia but no nuclear translocation of β-catenin can be observed in mALA+Light treated samples as compared to Light control samples. Bars: 50 µm. b) Immunoblot analysis of the indicated proteins in back skin samples showing no significant changes induced by mALA-PT in the phosphorylation levels on Thr180/Tyr182 of p38, Thr202/Tyr204 of p44/42 or Thr138/Tyr185 of JNK.

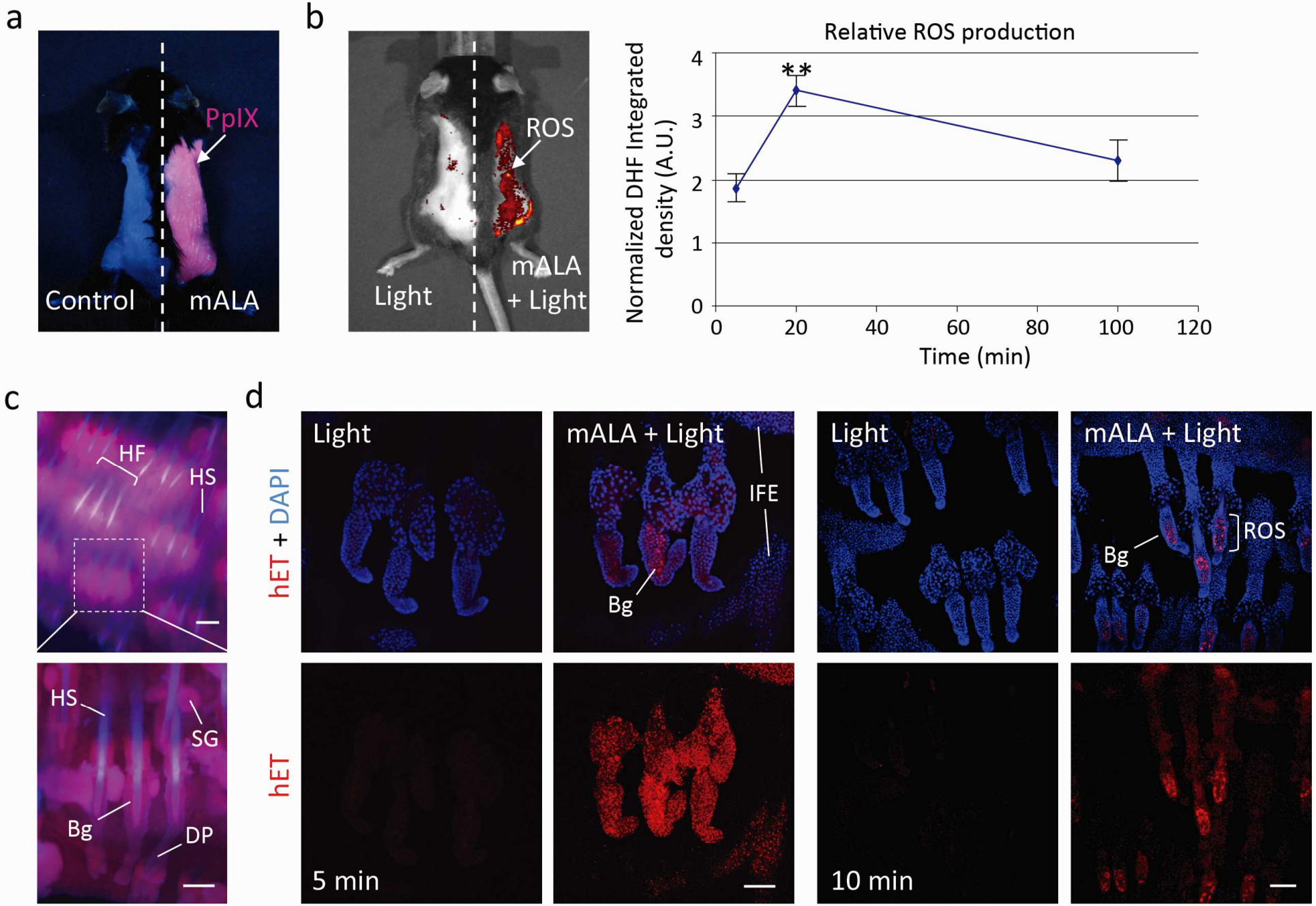

Figure 1. Carrasco et al. 2015

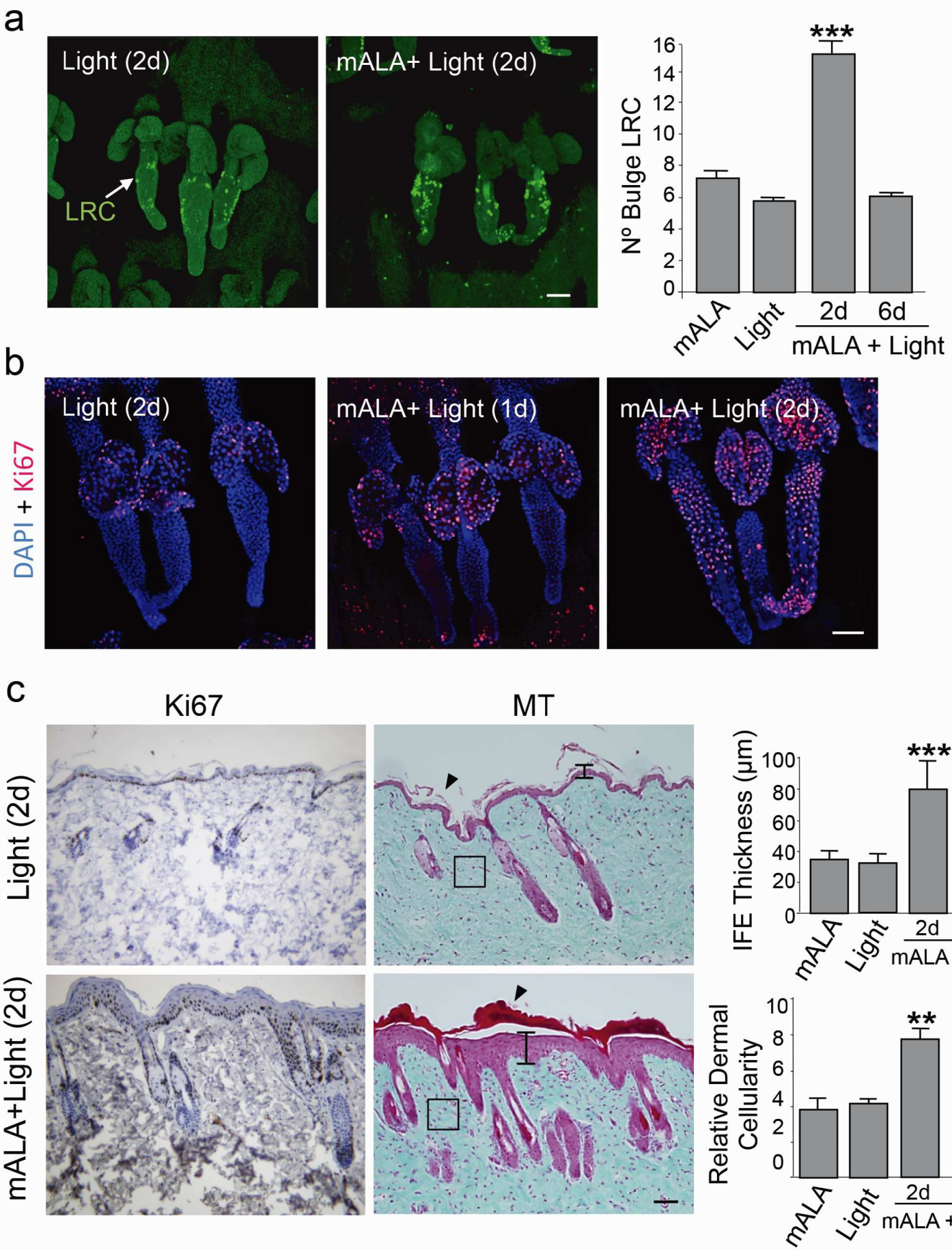

Figure 2. Carrasco et al. 2015

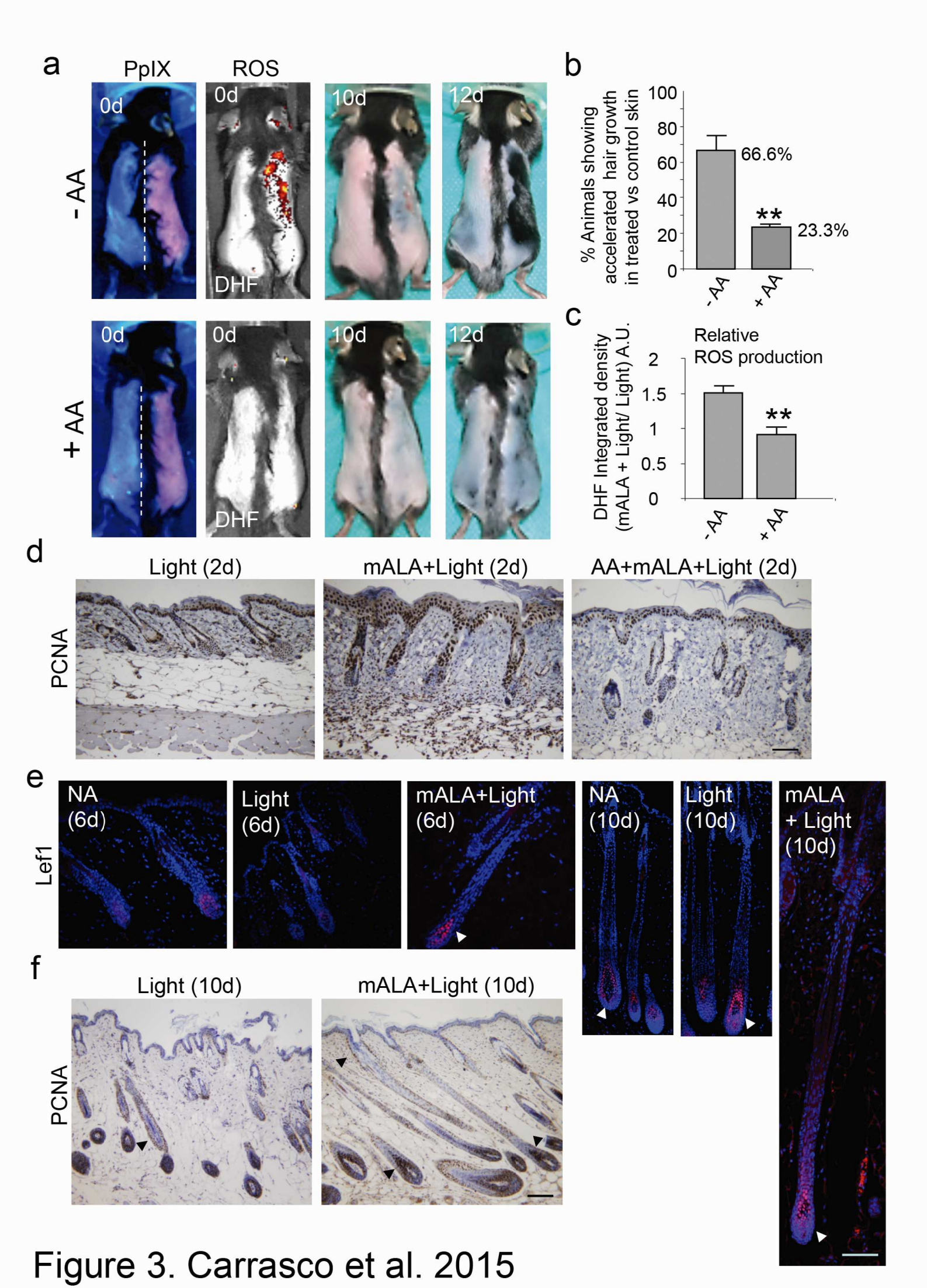

Figure 3. Carrasco et al. 2015

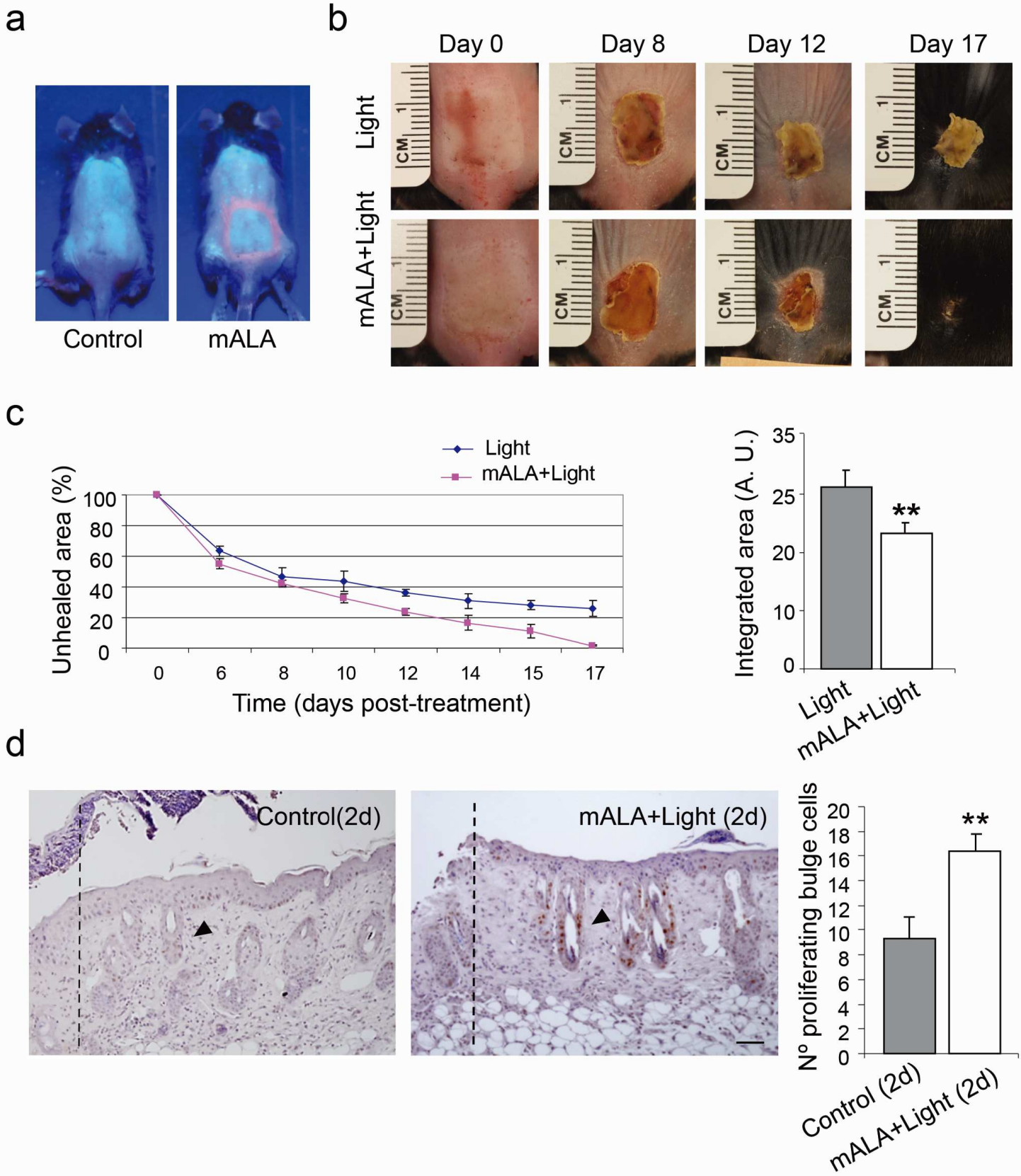

Figure 4. Carrasco et al. 2015

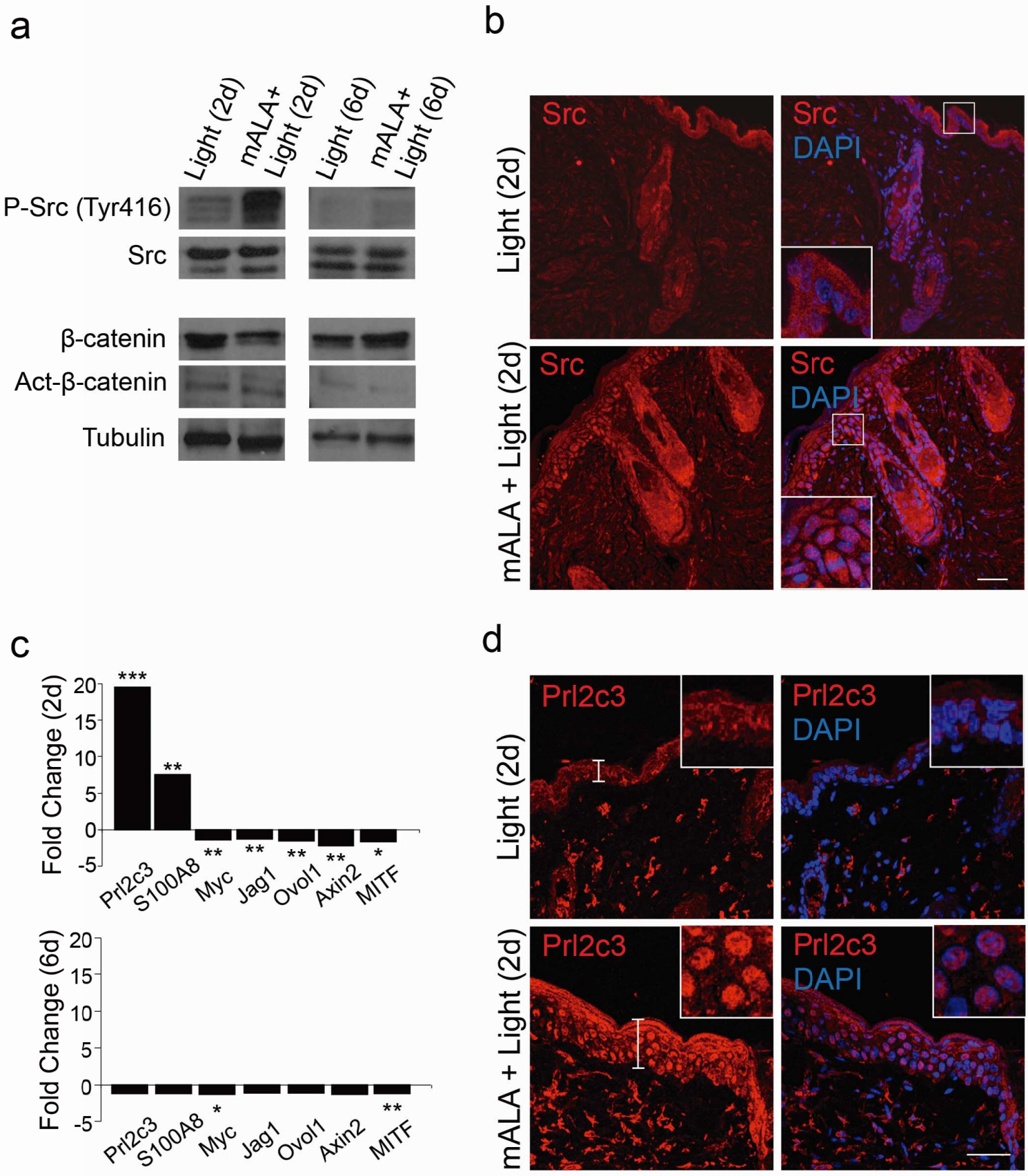

Figure 5. Carrasco et al. 2015

Gene	Access Nº GenBank	Expression ratio	Associated functions
Prl2c3	NM_011118	(+) 144.93	Hormone-like growth factor. Putative role in wound healing and hair follicle cycle.
S100a8	NM_013650	(+) 25.55	Calcium- and zinc-binding protein which has a wide plethora of intra- and extracellular functions, including the modulation of the NADPH-oxidase activity and a role as an oxidant scavenger, respectively.
Gsta4	NM_010357	(+) 21.24	Conjugation of reduced glutathione to a wide number of exogenous and endogenous hydrophobic electrophiles.
Hip1	NM_146001	(+) 16.78	Plays a role in clathrin-mediated endocytosis and trafficking. Proapoptotic protein. May be required for differentiation, proliferation, and/or survival of somatic and germline progenitors.
Sox5	NM_011444	(+) 11.73	TF that plays a role in cell lineage establishment during the development.
Fgf7 *(Kgf)*	NM_008008	(+) 4.40	Growth factor active on keratinocytes. Important role in the regulation of cell proliferation and differentiation.
Lef1	NM_010703	(+) 3.81	Participates in the Wnt signaling pathway. May play a role in hair cell differentiation and follicle morphogenesis.
Lrp1	NM_008512	(+) 3.15	Endocytic receptor involved in endocytosis and in phagocytosis of apoptotic cells. May modulate cellular events, such as kinase-dependent intracellular signaling.
Tln2	NM_001081242	(+) 3.11	Major component of focal adhesion plaques that links integrin to the actin cytoskeleton.
Gapdh	NM_008084	(+) 3.07	Has both glyceraldehyde-3-phosphate dehydrogenase and nitrosylase activities, thereby playing a role in glycolysis and nuclear functions, respectively.
Myh4	NM_010855	(+) 2.79	Muscle contraction.
Fgf18	NM_008005	(+) 2.38	Important role in the regulation of cell proliferation, cell differentiation and cell migration. Stimulates hepatic and intestinal proliferation.
Cdh11	NM_009866	(-) 2.62	Calcium-dependent cell adhesion protein (homophilic interactions).
Bmp2	NM_007553	(-) 3.14	Induces cartilage and bone formation.
Notch2	NM_010928	(-) 3.14	Functions as a receptor for membrane-bound ligands Jagged1, Jagged2 and Delta1 to regulate cell-fate determination.
Rora	NM_013646	(-) 3.16	Orphan nuclear receptor. Regulates a number of genes involved in lipid metabolism, in cerebellum and photoreceptor development in circadian rhythm and skeletal muscle development.
Myc	NM_010849	(-) 3.31	TF involved in the regulation of cell proliferation and cell differentiation of stem cells.
Mest	NM_008590	(-) 4.31	Belongs to the AB hydrolase superfamily. Expressed in mesodermal tissues.
Pcaf	AF254442	(-) 4.35	Functions as a histone acetyltransferase (HAT) to promote transcriptional activation.
Ikzf4	NM_011772	(-) 5.03	DNA-binding protein that binds to the 5'GGGAATRCC-3' Ikaros-binding sequence. Interacts with SPI1 and MITF.

Table 1. Carrasco et al. 2015

a

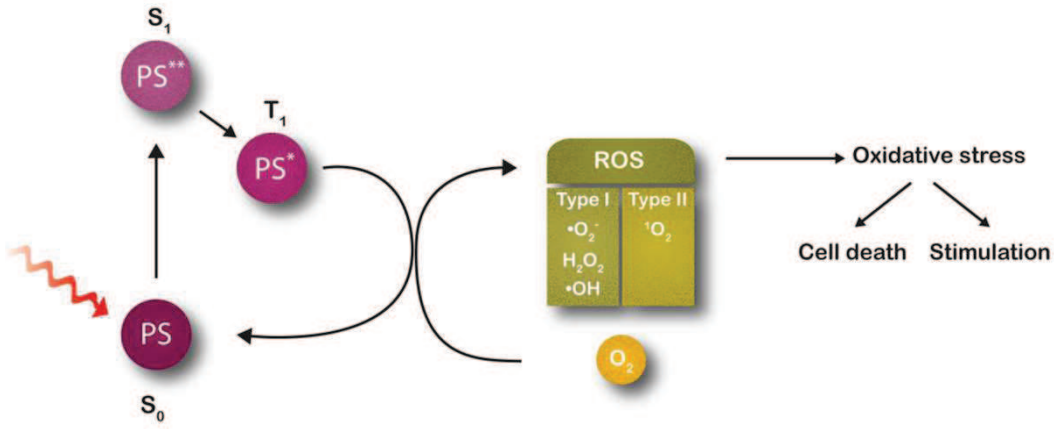

b

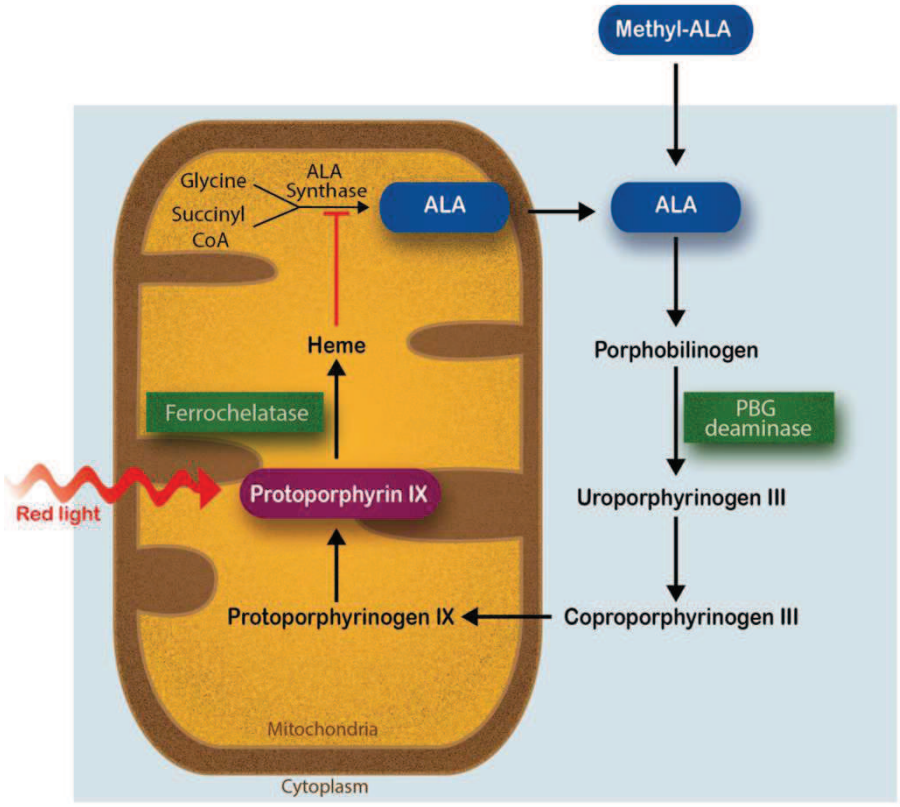

Figure S1. Carrasco et al. 2015

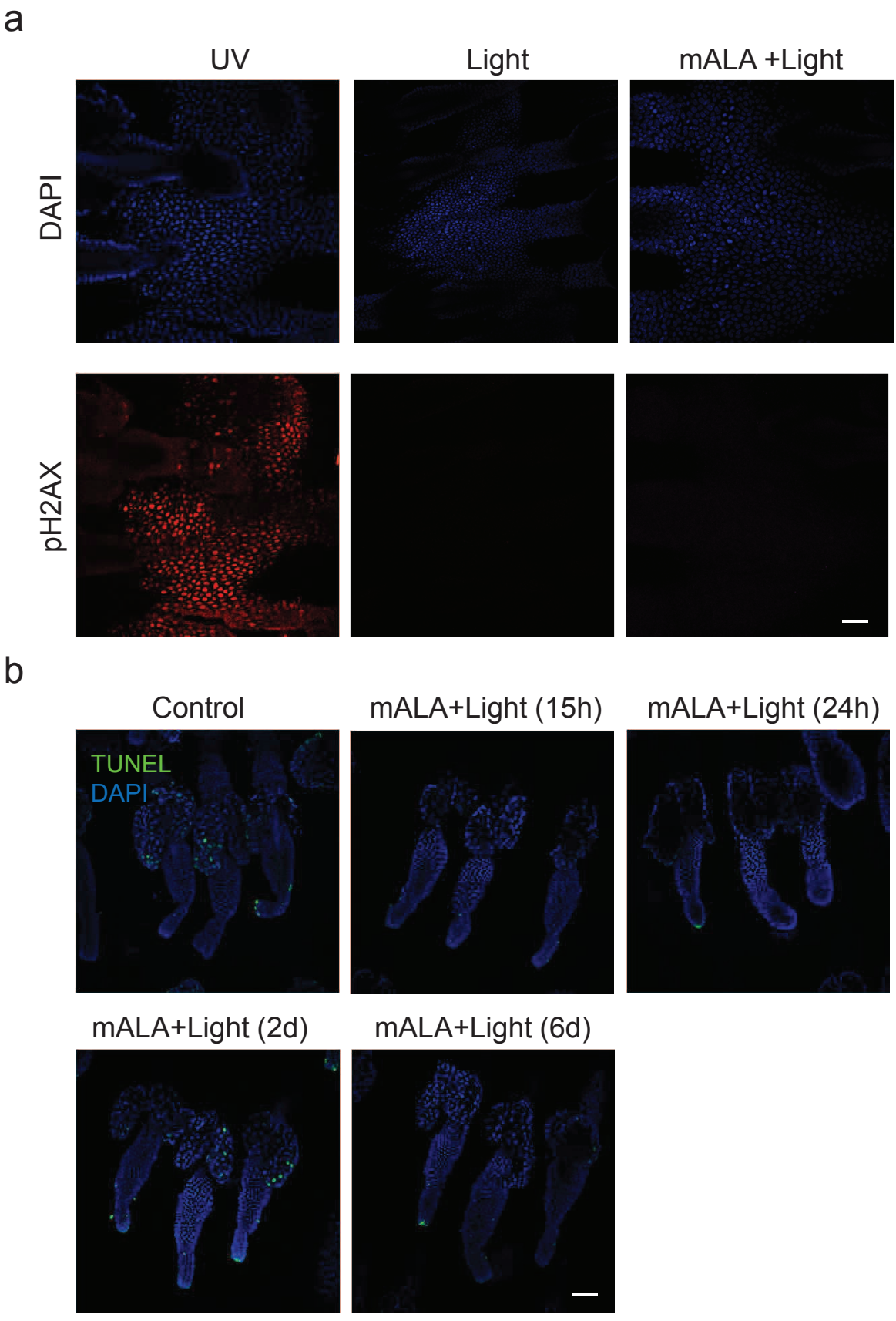

Figure S2. Carrasco et al. 2015

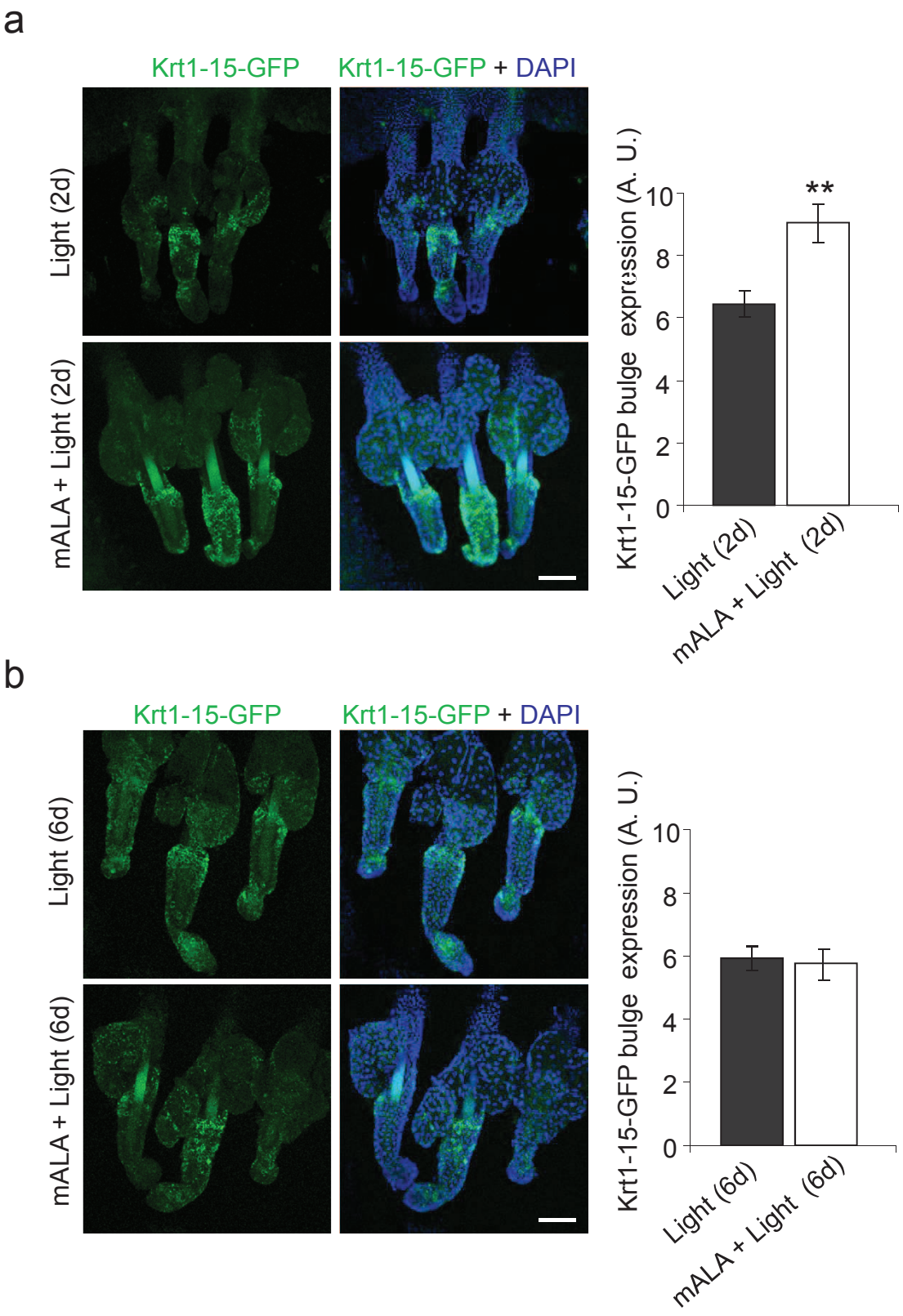

Figure S3. Carrasco et al. 2015

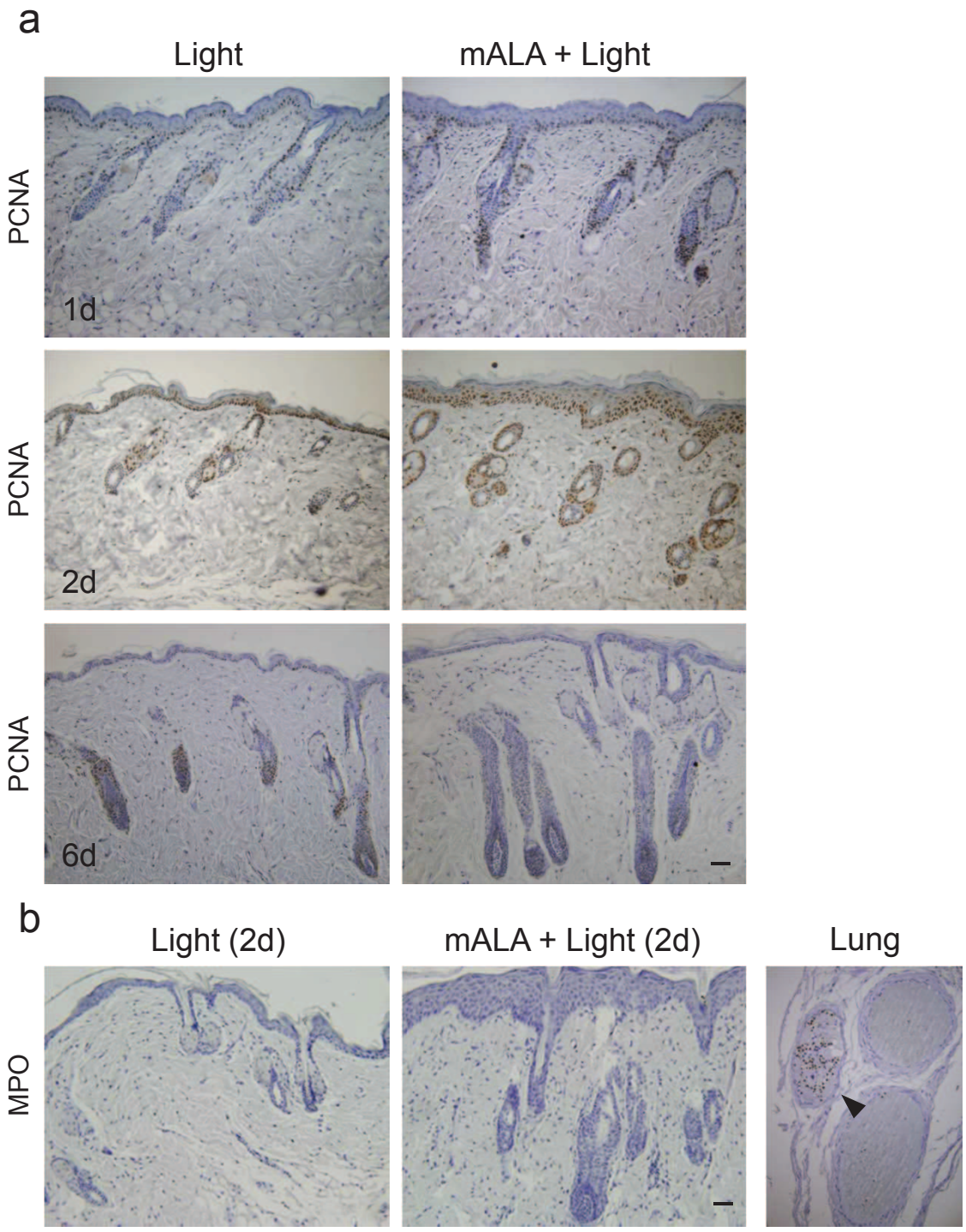

Figure S4. Carrasco et al. 2015

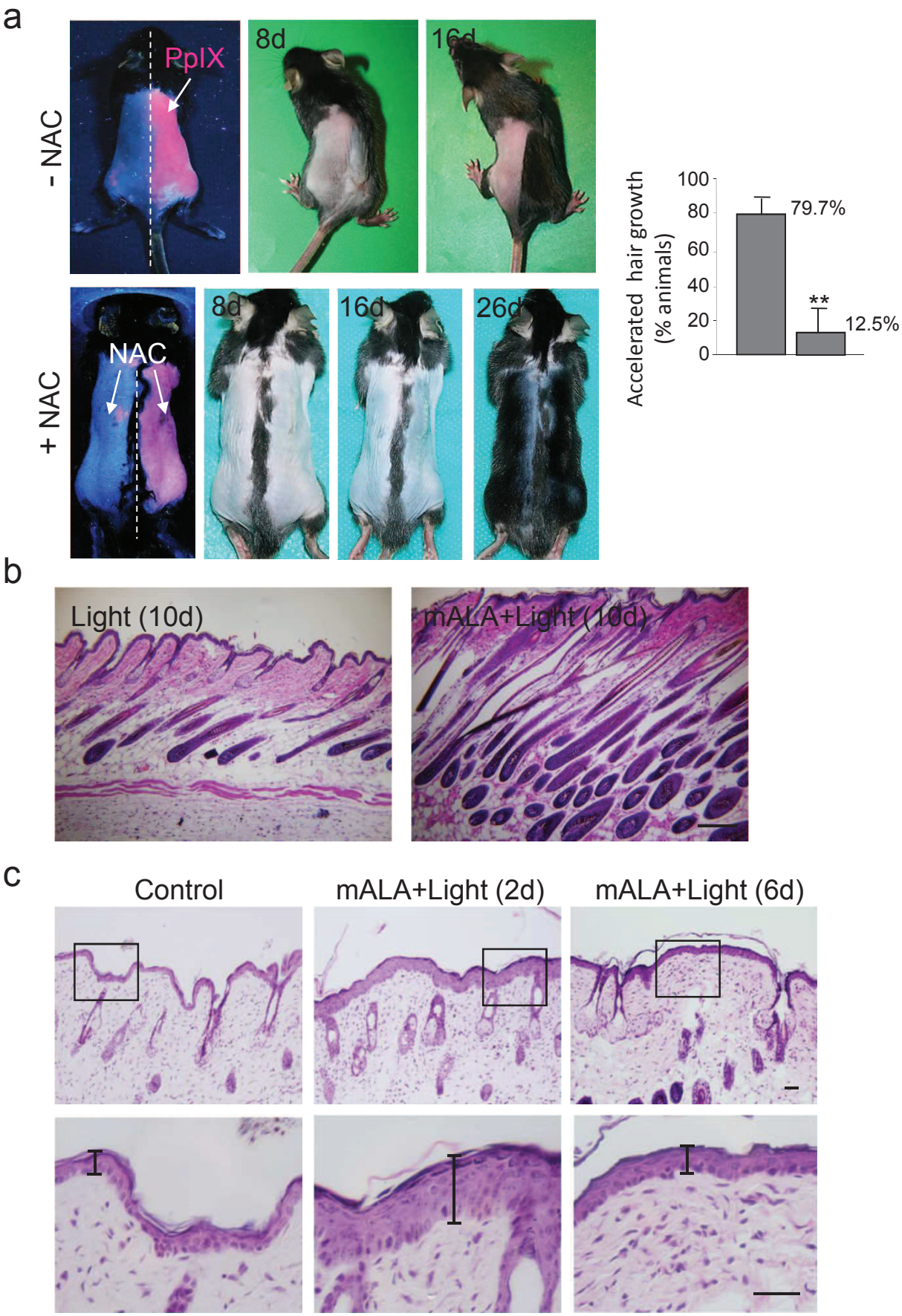

Figure S5. Carrasco et al. 2015

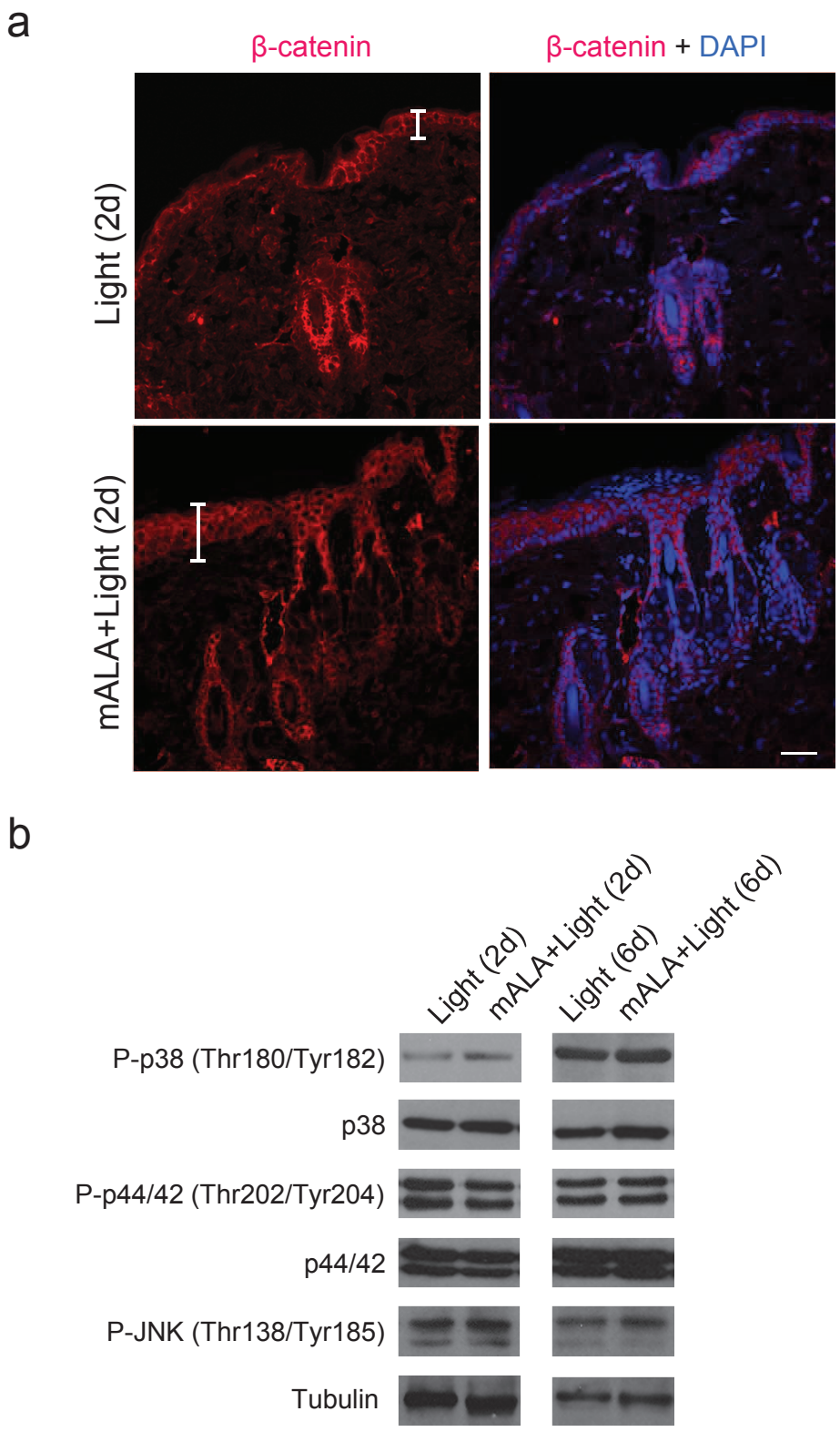

Figure S6. Carrasco et al. 2015